Osinga, H. M., Sherman, A., & Tsaneva-Atanasova, K. T. (2011). Cross-currents between biology and mathematics on models of bursting.

Early version, also known as pre-print

Link to publication record in Explore Bristol Research
PDF-document

University of Bristol - Explore Bristol Research
General rights

Cross-currents between biology and mathematics on models of bursting

HINKE M. OSINGA[a], ARTHUR SHERMAN[b] AND KRASIMIRA TSANEVA–ATANASOVA[a]

[a] Bristol Centre for Applied Nonlinear Mathematics
Department of Engineering Mathematics
University of Bristol
Bristol BS8 1TR, UK

[b] Laboratory of Biological Modeling
N.I.D.D.K. National Institutes of Health
12A SOUTH DR MSC 5621
Bethesda, MD 20892-5621

Abstract

A great deal of work has gone into classifying bursting oscillations, periodic alternations of spiking and quiescence modeled by fast-slow systems. In such systems, one or more slow variables carry the fast variables through a sequence of bifurcations that mediate transitions between oscillations and steady states. The most rigorous approach is to characterize the bifurcations found in the neighborhood of a singularity. Fold/homoclinic bursting, along with most other burst types of interest, has been shown to occur near a singularity of codimension three by examining bifurcations of a cubic Liénard system. Modeling and biological considerations suggest that fold/homoclinic bursting should be found near fold/subHopf bursting, a more recently identified burst type whose codimension has not been determined yet. One would expect that fold/subHopf bursting has the same codimension as fold/homoclinic bursting, because models of these two burst types have very similar underlying bifurcation diagrams. However, we are unable to determine a codimension-three singularity that supports fold/subHopf bursting. Furthermore, we believe that it is not possible to find a codimension-three singularity that gives rise to all known types of bursting. Instead, we identify a three-dimensional slice that contains all known types of bursting in a partial unfolding of a doubly-degenerate Bodganov–Takens point, which has codimension four.

1   Introduction

Fast-slow systems, particularly oscillators with fast activation and slow inhibition, are ubiquitous in biology (see, for example, [14]); this is likely because cells are replete with mechanisms on a wide range of time scales and because negative feedback is powerfully selected by evolution to maintain homeostasis. The combination of these ingredients leads naturally to oscillations that break away from homeostasis, i.e., lose stability by bifurcation, in order to support homeostasis on a longer time scale. When oscillations on different time scales become interlinked, bursting oscillations, which consist of alternating active and silent periods, often ensue.

Electrically excitable cells, such as neurons and secretory cells, display a wide variety of bursting rhythms. One reason is that single cycles of fast oscillations (spikes or action potentials) are ineffective at mediating the build-up of calcium, which is needed to trigger release of neurotransmitters and hormones. A particularly favorable form of bursting for this purpose is *plateau bursting*, which provides a prolonged period of high membrane potential to mediate calcium entry [9]. Plateau bursting both resembles and shares features of mathematical structure with relaxation oscillations, but the excited, high-voltage state is adorned with small-amplitude spikes.

The first mathematical models for bursting were guided by this simple intuition of spike trains modulated by a slow process. An early fruitful example was the model for insulin-secreting pancreatic beta cells of Chay and Keizer [4]. Rinzel [18] pioneered the bifurcation analysis of these systems, showing that such bursts could be generated by a so-called frozen system or fast subsystem that had bi-stability between a low-voltage steady state and a high-voltage spiking state. Upward transitions were initiated by a saddle-node bifurcation and downward transitions by passage through a homoclinic orbit. A simple example of such a burster, informally called a square-wave burster, is shown in Figure 1(a) and the corresponding bifurcation diagram in Figure 1(b). Rinzel also began the process of classifying the various burst patterns that were emerging at that time in terms of the bifurcations marking the transitions [19].

Another formative example was the bursting observed in R15 neurons of the sea snail *Aplysia*, which is characterized by a spike frequency that first increases and then decreases during the active (spiking) phase [1]. This was dubbed parabolic bursting and was elegantly demonstrated to be explained by passage in the frozen system through a curve of saddle-node-on-invariant-circle (SNIC) bifurcations at both the beginning and end of the active phase [21]. A model for a third form of bursting, observed in an oscillating chemical reaction, was shown to be mediated by bi-stability generated by a subcritical Hopf bifurcation [19]. Hoppensteadt and Izhikevich [12] pointed out that there should be many more burst types, sixteen if one considers just the bifurcations of planar fast subsystems that can mediate transitions between fixed points and limit
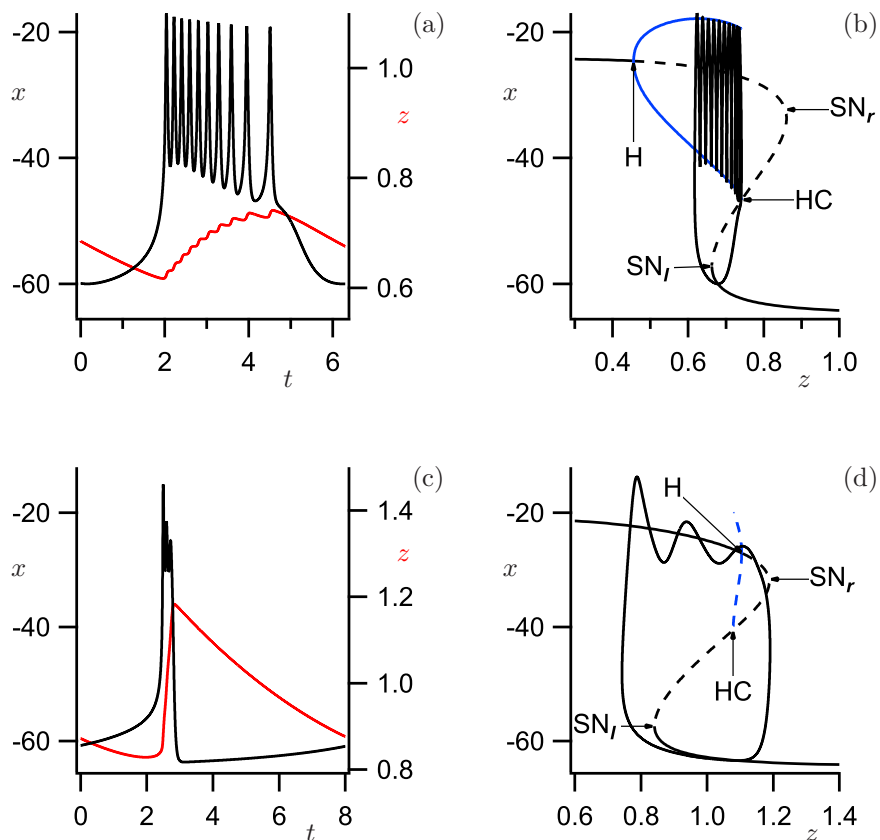
Figure 1: Time series (a) and bifurcation diagram (b) for square-wave (fold/homoclinic) bursting in a conductance-based model. Time series (c) and bifurcation diagram (d) for pseudo-plateau (fold/subHopf) bursting. Parameters as in [27, Fig. 1], except that here the square-wave bursting trajectory is calculated for $f_c = 0.0052$.

cycles, and up to 120 if one defines bursting more broadly. In their nomenclature, square-wave bursting became "fold/homoclinic" bursting.

These early successes in modeling and in classifying the diverse patterns prompted an ongoing effort to ascertain mathematically what other burst types might exist and what are the simplest mathematical models that can instantiate them. Cells perform vastly different tasks and so diversity is to be expected as cells randomly explore the bifurcation landscape. Simplicity, on the other hand, is not a priority for Nature and,

indeed, redundancy is generally preferable in order to buffer cells from imperfections such as noise and heterogeneity in the components at their disposal, as well as provide sites of regulation. Nonetheless, it has been both of mathematical and biological interest to know what the limits of such exploration are.

One type of bursting that was not appreciated at the time of previous classification efforts is that of fold/subHopf bursting, shown in Figures 1(c) and (d); in contrast to the bifurcation diagram in Figure 1(b) that corresponds to square-wave bursting, the Hopf bifurcation for fold/subHopf bursting is subcritical. This type of plateau bursting had, in fact, been predicted as a missing element in the tables of Hoppensteadt and Izhikevich [12, 13], but did not show up in a biophysical model until the papers by Tsaneva-Atanasova *et al.* [28] and Stern *et al.* [23] on pituitary somatotrophs. (Van Goor *et al.* [8] had previously published a model for somatotrophs with this bifurcation structure but did not show the bifurcation diagram.) Fold/subHopf bursting had been overlooked because its appearance as in Figure 1(c) is similar to that of square-wave bursting in Figure 1(a), except for the suspiciously small spike amplitude. However, hewing closely to the data revealed the fold/subHopf structure and showed that the small spike amplitude was a consequence of not having any stable limit-cycle attractors in the frozen system. The spikes then are only seen if the speed ϵ of the slow variable is not very small. This seems paradoxical, as bursting trajectories were previously understood to be a sequence of states of the system that exist in the limit $\epsilon \to 0$ and are visited as the slow variable(s) evolve in time. In contrast, the states visited during fold/subHopf bursting are transients of the frozen system, not attractors. As shown in Figure 1(d) at the end of the active phase, the plateau can persist even when there is no stable solution at all. Such bursting with transient spikes has been called *pseudo-plateau* bursting to distinguish it from square-wave bursting [23]. Cells, not being scrupulous about observing the neat formulations of mathematicians, readily exploit the fold/subHopf structure, which has now turned up in models for another pituitary cell, the lactotroph [24, 26].

In this paper we follow [2, 7] and investigate the complexity of burst types in terms of the codimension of the singularity in whose unfolding it first appears. We briefly recall this approach in the next section and discuss that most known burst types are found in the codimension-three unfolding of a degenerate Bogdanov–Takens point. However, we do not expect to find fold/subHopf bursting alongside these other known burst types; we explain this in Section 3, where we focus our attention on a partial unfolding of a *doubly*-degenerate Bogdanov–Takens point as studied in [15]. We are able to identify almost all known burst types in a neighborhood of this codimension-four singularity. We end with conclusions in Section 4.

2 Towards a normal form for bursting

In the original Chay–Keizer model [4] the four equations of the classical Hodgkin–Huxley system [11] were modified to provide for a parameter regime with three steady states, and an equation for calcium was added. It was quickly realized that two variables could be set to equilibrium, leaving two variables to mediate spiking and one for negative feedback, leading to equations of the form

$$\begin{cases} \dot{x} &= f(x, y, z), \\ \dot{y} &= \phi\, g(x, y), \\ \dot{z} &= \varepsilon\, h(x, z). \end{cases} \tag{1}$$

This is the minimum number of equations for bursting; some types, such as parabolic bursting, require a second slow variable [19, 21]. The parameter ϕ has to be sufficiently small to yield spiking, and ε has to be much smaller than ϕ to allow for multiple spikes per burst. Figure 1 shows examples of fold/homoclinic and fold/subHopf bursting for a model that was made using the Hodgkin–Huxley formalism, with x representing membrane potential, y activation of a voltage-dependent potassium current, and z cytosolic calcium; the slow rise in calcium acts on a calcium-activated potassium channel to terminate the active phase. We used the equations and parameters as in [27, Fig. 1], except that $f_c = 0.0052$ for the square-wave bursting shown in Figures 1(a) and (b). Figures 1(a) and (c) show the time series of x and z for both square-wave and pseudo-plateau bursting, respectively; in panels (b) and (d) the respective bursting orbits are overlaid on the bifurcation diagrams that are obtained by considering only the (x, y)-equations in (1) and using the slow variable z as a bifurcation parameter.

If one is willing to give up biophysically identifiable ion currents then the functions f, g, and h in (1) can be replaced by polynomials. Hindmarsh and Rose [10] adopted for f the cubic of the Fitzhugh–Nagumo system, originally introduced as a model for simple spiking, which allows for three steady states. They found, however, that g needed to be quadratic to break the symmetry between the upper and lower states, allowing one to be a fixed point and the other a limit cycle. The function h need only be linear.

2.1 Classification of Bursters by Unfolding

The next advance in classification was by Bertram *et al.*, who showed that the three burst patterns identified by Rinzel could be located in a single two-parameter bifurcation diagram [2]; they identified one parameter (which we denote μ_1 in this paper) with the slow negative feedback variable (which represents z above) and the other (corresponding to ν in this paper) a parameter of the two-dimensional frozen system involving only the equations for x and y above. Bertram *et al.* pointed out that the two-parameter plane

in [2, Fig. 7] was a slice of the unfolding of a codimension-three singularity, namely, a degenerate Bogdanov–Takens point of focus type; this singularity had been studied by Dumortier *et al.* [6], who were not concerned about bursting but sought to categorize all singularities of planar vector fields.

Apart from unifying the known burst patterns, [2, Fig. 7] revealed two additional types of bursting that emerged naturally as the parameter corresponding to ν was varied. One of these was a second type of fold/homoclinic burster that did not take the form of a square wave because the limit cycles surrounded all three steady states. This burst type had previously been found by Pernarowski [17] in a cubic Liénard system augmented by a slow variable and described as "nearly parabolic" bursting, because of the large-amplitude spikes that turned out not to involve passage across a SNIC; it is called type Ib in [2, 7] to distinguish it from the classical fold/homoclinic bursting with square-wave appearance (historically, type I). The bifurcations of the cubic Liénard system were later systematically studied by De Vries [30].

The work in [2] suggested that additional types of bursters were possible and that unfolding would be a way to find and classify them. This approach was taken up by Golubitsky *et al.* [7], who pointed out that unfolding would also provide an unambiguous way to define the complexity of a burst type in terms of the codimension of the singularity in whose unfolding it first appears. They showed, in particular, that fold/homoclinic bursting appears for the first time in the unfolding of a codimension-three singularity, namely, exactly the degenerate Bogdanov–Takens point studied in [6]. Golubitsky *et al.* [7] used the following normal form

$$\begin{cases} \dot{x} & = & y, \\ \dot{y} & = & \mu_1 + \mu_2\, x - x^3 + y\,(\nu + b\, x + x^2), \end{cases} \qquad (2)$$

with $b = 3$, which puts the system into the elliptic case studied in [6], rather than the focus case. Nonetheless, they were able to identify a path for fold/homoclinic bursting in the (μ_1, ν)-plane with $\mu_2 = \frac{1}{3}$ fixed. Parabolic bursting could be obtained by choosing a different path in this same plane. Rinzel's subHopf/fold-cycle burster, in contrast, was determined to have codimension two.

3   Partial unfolding of a codimension-four singularity

One blemish on the fold/homolinic burst path identified by Golubitsky *et al.* [7] is that system (2) exhibits an unstable limit cycle of large amplitude that surrounds the region in phase space that is involved in the burst; this is not seen in the biophysical models.

This blemish can be removed by considering the focus case in [6], that is, choosing $b < 2\sqrt{2}$ in (2), but then time must be reversed, which also reverses the orientation of μ_1, ν and x. The reversal of time exchanges the criticality of the Hopf bifurcations and the supercritical Hopf bifurcation needed for fold/homoclinic bursting is now located in a parameter regime where no large surrounding periodic orbits exist. By reversing time, the equations take the form used by Khibnik *et al.* [15], who studied a partial unfolding in cubic Liénard form of a doubly-degenerate Bogdanov–Takens bifurcation. We write this partial unfolding as:

$$\begin{cases} \dot{x} & = & y, \\ \dot{y} & = & -\mu_1 + \mu_2\,x - x^3 + y\,(\nu + b\,x - x^2). \end{cases} \tag{3}$$

That is, we renamed the parameters $(\mu_1, \mu_2, \mu_3, \mu_4)$ in [15] as $(-\mu_1, \mu_2, \nu, b)$. (Note that we use the notation $-\mu_1$ rather than μ_1 in order to achieve consistency with the orientation of the slow variable z.)

The origin $(\mu_1, \mu_2, \nu, b) = (0, 0, 0, 0)$ is the doubly-degenerate Bogdanov–Takens bifurcation point, but as discussed in [15], the focus case of [6] can be found by taking a slice with $0 < b < 2\sqrt{2}$ fixed. Due to the conic structure of the bifurcation diagram in these high-dimensional parameter spaces it suffices to study the bifurcations on the boundary of a codimension-one sphere of small enough radius, which after stereographic projection leads to the planar bifurcation diagrams shown in [6, 15] that represent the (μ_1, μ_2, ν)-space with b fixed. More precisely, the focus case in [6] is reproduced as case (M) in [15, Fig. 5]. Case (M) is the last image in a series of b-slices depicted in Figs. 4 and 5 of [15] to illustrate a possible path from the local bifurcation structure near $(\mu_1, \mu_2, \nu) = (0, 0, 0)$ with $b = 0$, which is case (A) in [15, Fig. 4], to the local bifurcation structure as we know it for the focus case with $0 < b < 2\sqrt{2}$. The intermediate bifurcation diagrams indicate the presence of other codimension-three singularities that must be expected nearby in a neighborhood of $(\mu_1, \mu_2, \nu, b) = (0, 0, 0, 0)$; if the radius of the sphere were chosen small enough, one would recover the bifurcation diagram for the focus case for any $0 < b < 2\sqrt{2}$. In the series of bifurcation diagrams for fixed b, Khibnik *et al.* indicate only one case that would support both fold/homoclinic (square-wave) and fold/subHopf (pseudo-plateau) bursting, namely, case (I) in [15, Fig. 4].

In our quest to find a path for pseudo-plateau bursting, we computed bifurcation diagrams on the unit sphere for various choices of b decreasing from $b = 3$; we used the same parameterization described in the on-line supplement to [15]. Figure 2 shows the bifurcation diagram for $b = 0.75$ as the closest resemblance to case (I); unfortunately, the series of codimension-three bifurcations is not quite as suggested by Khibnik *et al.* [15]. The bifurcation diagram in Figure 2 does support pseudo-plateau bursting, which is defined by a path segment that crosses both saddle-node bifurcations (SN_l and SN_r) at the left and right knees of the regime with three steady states such that it only
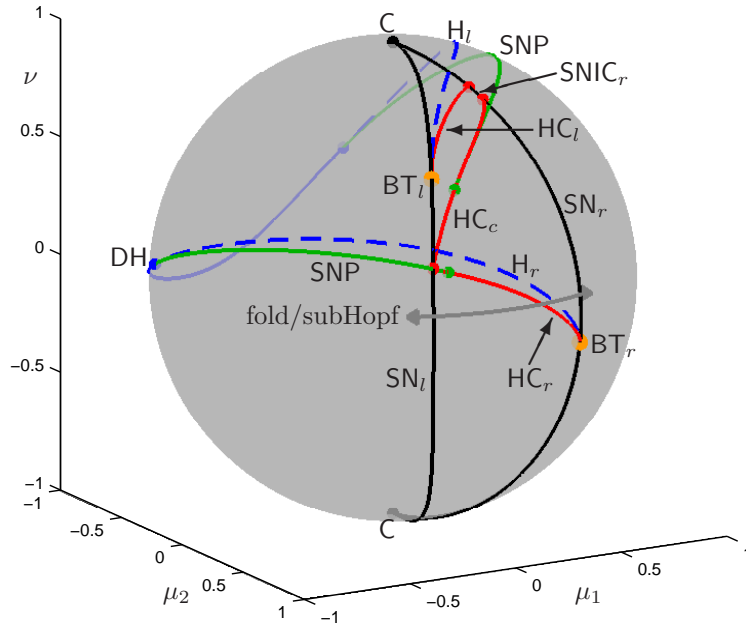
Figure 2:   Bifurcation diagram of system (3) with $b = 0.75$ on the unit sphere in (μ_1, μ_2, ν)-space.   Color in on-line version: red, homoclinic (HC); blue, Hopf bifurcation (H; solid: supercritical, dashed: subcritical); black, saddle-node (SN); orange, Bogdanov–Takens point (BT); green, saddle node of periodics (SNP); degenerate Hopf and cusp are labeled DH and C, respectively.   A path of pseudo-plateau bursting is indicated; we used the circle segment on the unit sphere with $\nu = 0.1$ and $\mu_1 = \sqrt{1 - \nu^2} \cos(2\pi\vartheta)$, where ϑ varies between 0.245 ± 0.065.

intersects the curves of homoclinic (HC_r) and subcritical Hopf bifurcations (H_r) that emanate from the right Bogdanov–Takens point (BT_r). However, there is no path on the sphere in Figure 2 that would represent square-wave bursting. For this, the curve H_r from BT_r must become supercritical before it crosses the homoclinic HC_c, that is, DH should lie between SN_l and SN_r.

As mentioned above, the unfolding of the codimension-three degenerate Bogdanov–Takens point at $(\mu_1, \mu_2, \nu) = (0, 0, 0)$ with $b = 0.75$ is like that of the focus case in [6], that is, case (M) in [15, Fig. 5]. We would recover the bifurcation diagram of the focus case if we decrease the radius of the sphere shown in Figure 2 enough such that it does not enclose other codimension-three singularities. To see this, we compute the bifurcation

diagram of (3) for $b = 0.75$ and $\mu_2 = 0.0675$ fixed. This (μ_1, ν)-plane is shown in Figure 3; its location in (μ_1, μ_2, ν)-space relative to the unit sphere of Figure 2 is shown in Figure 3(a) and the slice itself in panel (b). All ingredients that are important for the bifurcation structure on this slice are present in a small neighborhood of the origin $(\mu_1, \nu) = (0, 0)$, which is also a small neighbhorhood of the origin in (μ_1, μ_2, ν)-space, since $\mu_2 = 0.0675$ is small; an enlargement of this neighborhood is shown in Figure 3(c), where we can again capture fold/homoclinic bursting for a path segment that crosses SN_l and SN_r such that it only intersects the curves HC_r and H_r that emanate from BT_r; this is so, because H_r is now supercritical, as is required for the focus case. Note the similarity of Figure 3(c) with [2, Fig. 7] and [30, Fig. 18], but with the top-down orientation reversed.

In fact, as in [2, 30], we can choose horizontal path segments with ν constant and μ_1 playing the role of the slow variable. For ν-values between the minimum of HC_r and the bottom of the SNIC region SNIC_l we get square-wave bursting. Note that the Hopf bifurcation required for square-wave bursting occurs (far) to the left of SN_l in Figure 3; if both Hopf bifurcations lie between SN_l and SN_r, which happens if the minimum of H_r lies between SN_l and SN_r, then the spike envelope of the burst first shrinks in amplitude then grows. This was termed "parabolic amplitude bursting" in the Liénard model of Pernarowski [17, Fig. 1(c)] and was also found in a Hodgkin-Huxley model for pituitary corticotrophs [16]. Mathematically, these cases are topologically equivalent and also from a physiological point of view, the latter is considered a minor variant of fold/homoclinic bursting because it does not involve any differences in the bifurcation structure.

Moving ν up so that horizontal trajectories cross SNIC_l gives parabolic bursting; and moving ν further up to cross the middle homoclinic curve HC_c gives fold/homoclinic with large limit cycles. Other bursters with large limit cycles are found as ν is increased further, as described in detail in [2].

If ν is chosen below the minimum of HC_r but above the minimum of H_r, there are two Hopf bifurcations on the upper steady-state branch of the frozen system that are joined by a closed curve of periodic orbits. The shape of the active-phase spike envelope again depends on whether both Hopf bifurcations on H_r occur between SN_l and SN_r or one lies to the left of SN_l. The latter is the case in Figure 3 and results in tapered bursting; see, for example, [17, Fig. 1(e)] and [5, Fig. 7]. An example with both Hopf bifurcations between the knees is given in [25, Fig. 2]. In the nomenclature of Izhikevich and Hoppensteadt [12, 13] these are both variants of fold/fold bursting, which also occurs for ν-values below the minimum of H_r, when there are no longer any limit cycles in the frozen system. In the limit $\epsilon \to 0$, this last case is just a classic relaxation oscillator, but if ϵ is not very small compared to the rate of attraction to the upper stable steady state, spikes can appear on the plateau.
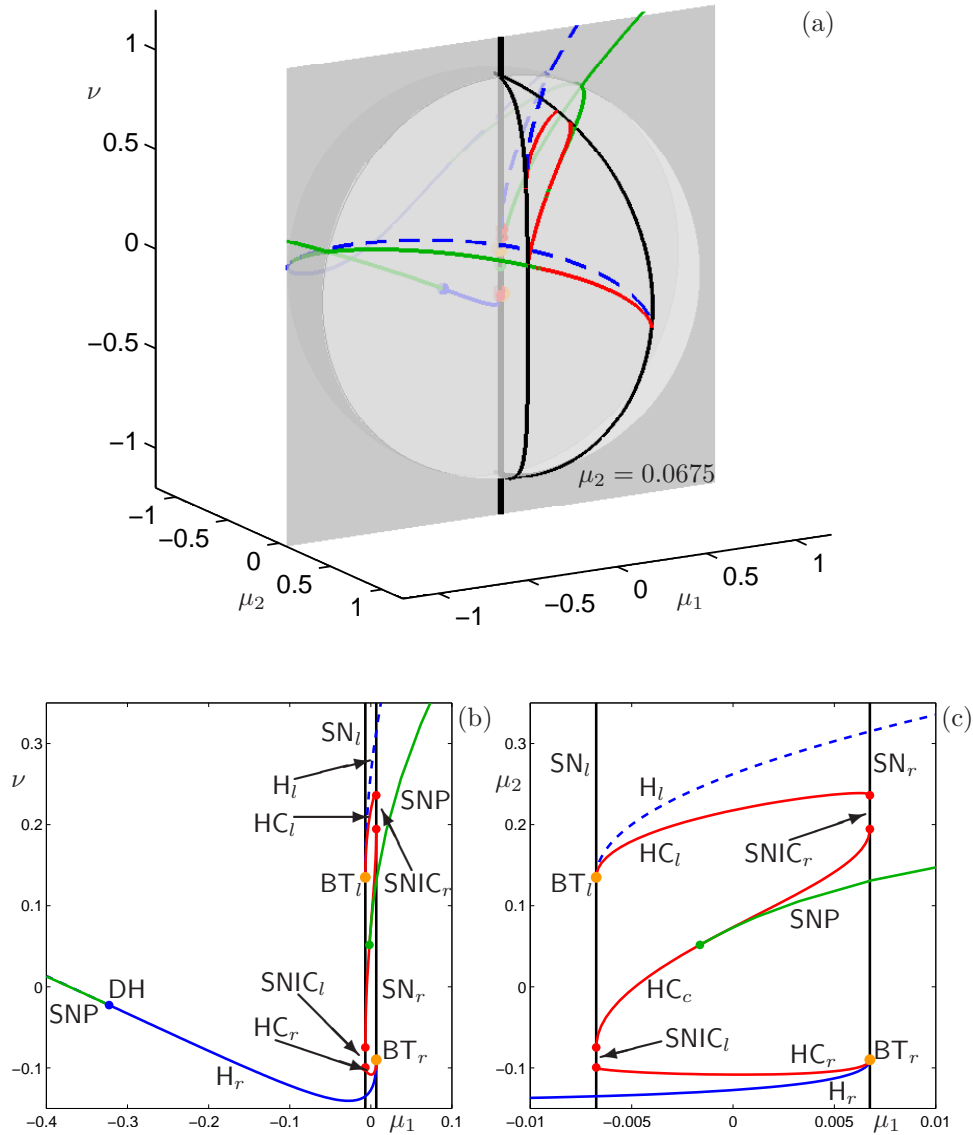
Figure 3:   Bifurcation diagram of (3) with $b = 0.75$ and $\mu_2 = 0.0675$; the bifurcation diagram on the unit sphere with $b = 0.75$ from Figure 2 is shown for reference in panel (a) with the (μ_1, ν)-plane shown in panel (b) and an enlargement in panel (c). Colors and symbols as in Figure 2.

We emphasize here that the location of the Hopf bifurcations relative to the knees is only of phenomenological interest. All of the burst types discussed above can be found in Figure 3, provided one allows for curved paths. Nonetheless, because of the ability to identify μ_1 with the slow variable and ν with a single parameter of the frozen system, it is rather easy to identify parameter regimes for the focus case of (3) that correspond to the wide range of burst types reported in the literature. In fact, these account for almost all the ones that have been found in models. There is no apparent way, however, to get fold/subHopf bursting in the slice represented in Figure 3. Yet, biologically one expects the cells they are found in (or at least in models thereof), to be closely related to both pituitary corticotrophs and pancreatic β cells. Also, the fold/homoclinic and fold/subHopf bursters shown in Figure 1 were obtained from the same model by changing a single parameter, namely, one that controls the activation of the calcium current. Shifting this activation to lower voltages has the consequence that greater activation of the calcium-activated potassium channels is needed to destabilize the steady, high-voltage plateau. This shifts the Hopf bifurcation in Figure 1(b) to the right and also causes it to flip from supercritical to subcritical, i.e., it passes through a degenerate Hopf bifurcation. It was shown in [25] that shifting the activation of the voltage-dependent potassium channel causes the same transition, which, thus, seems easily available to cells.

We can obtain such a transition in the normal form (3), by taking a slice with fixed ν, rather than fixed μ_2. The bifurcation diagram of (3) with $b = 0.75$ and $\nu = -0.09$ is shown in Figure 4 using the same visualizations as in Figure 3; the location of the (μ_1, μ_2)-plane in (μ_1, μ_2, ν)-space relative to the unit sphere of Figure 2 is shown in panel (a), the slice itself in panel (b), and an enlargement in panel (c). Note that there are two Bogdanov–Takens points on SN_r in this slice, denoted BT_r and $\mathsf{BT}_r^{\mathrm{far}}$. Locally near the origin $(\mu_1, \mu_2) = (0, 0)$ we recognize part of the unfolding of the focus case [6, 15]; in fact, ν is chosen such that BT_r is exactly the same point BT_r in Figure 3. The transition from square-wave to pseudo-plateau bursting is organized by $\mathsf{BT}_r^{\mathrm{far}}$. From $\mathsf{BT}_r^{\mathrm{far}}$ emanates a subcritical Hopf bifurcation H that becomes supercritical at the point DH that lies just to the right of where H crosses SN_l; the degenerate Hopf bifurcation DH gives rise to a curve of saddle-nodes of periodics (SNP) that ends when it merges with the curve of homoclinics HC, which also emanates from $\mathsf{BT}_r^{\mathrm{far}}$.
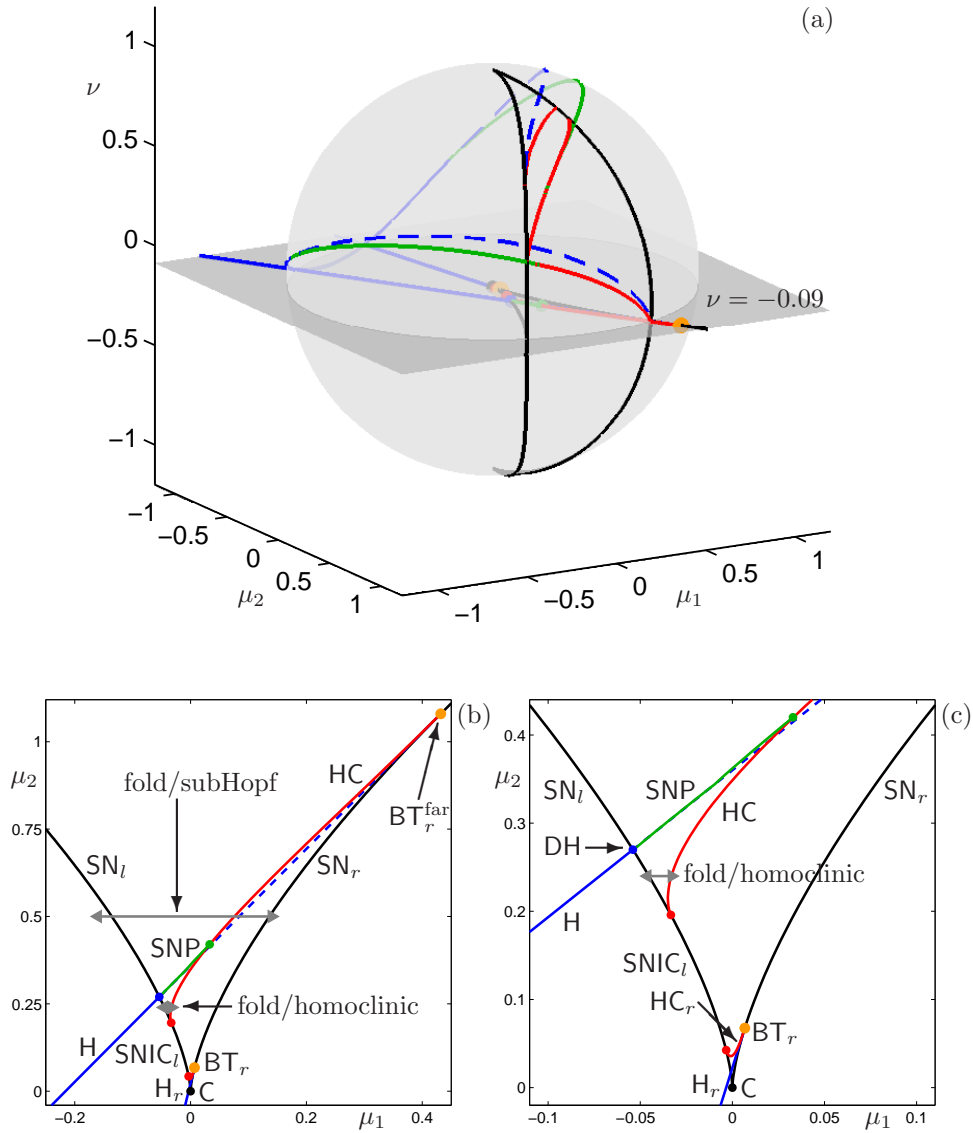
Figure 4: Bifurcation diagram of (3) with $b = 0.75$ and $\nu = -0.09$; the bifurcation diagram on the unit sphere with $b = 0.75$ from Figure 2 is shown for reference in panel (a) with the (μ_1, μ_2)-plane shown in panel (b) and an enlargement in panel (c). Note that there are two Bogdanov–Takens points, BT_r and $\mathsf{BT}_r^{\mathrm{far}}$, on the same side SN_r of the cusp point C; the point BT_r is also contained in the μ_2-slice shown in Figure 3. Two burst paths are indicated, which are the fold/subHopf and fold/homoclinic bursters illustrated in Figure 5. Colors and symbols as in Figure 2.
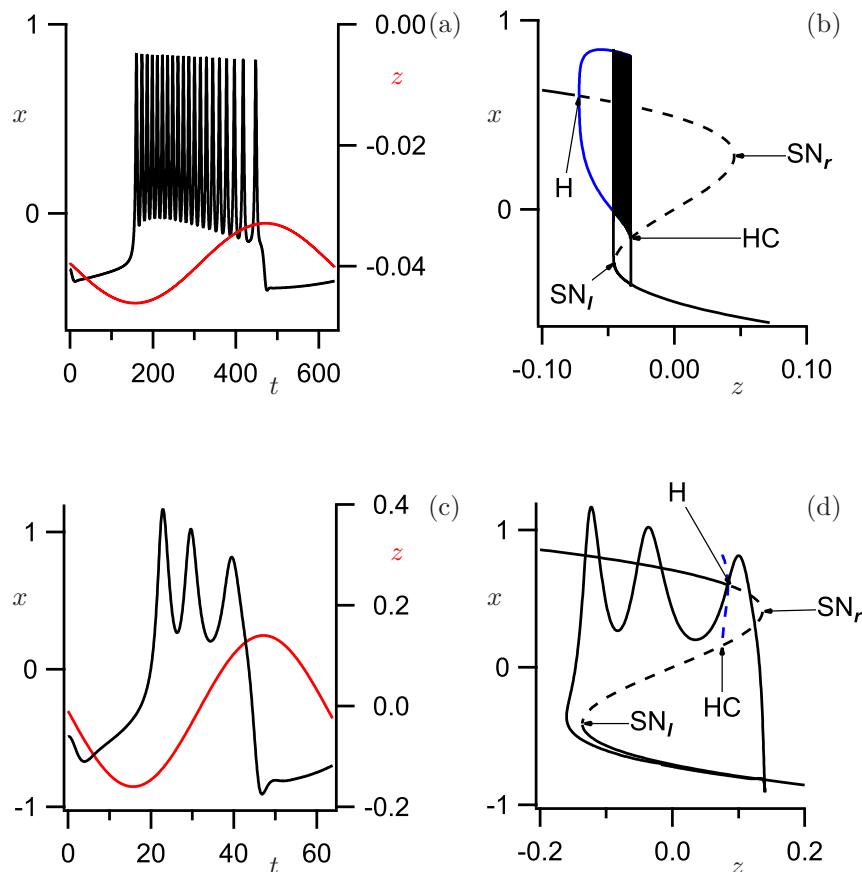
Figure 5: Time series and one-parameter bifurcation diagrams illustrating the two path segments indicated in Figure 4; we used (3) with $b = 0.75$ and $\nu = -0.09$, and $\mu_2 = 0.24$ for square-wave bursting in panels (a) and (b), and $\mu_2 = 0.5$ for pseudo-plateau bursting in panels (c) and (d), respectively. The parameter μ_1 acts as the slow variable z as defined in (4); we used $\bar{\mu}_1 = -0.0395$, $A = 0.0066$ and $\varepsilon = 0.01$ for $\mu_2 = 0.24$, and $\bar{\mu}_1 = -0.01$, $A = 0.15$ and $\varepsilon = 0.1$ for $\mu_2 = 0.5$.

Fold/homoclinic (square-wave) bursting can be obtained via a horizontal path segment with μ_2 fixed such that it lies below DH, but above the segment SNIC_l on SN_l. Figure 5(a) shows an example of such a time series for x and z with $\mu_2 = 0.24$, and Figure 5(b) shows the corresponding one-parameter bifurcation diagram. Here, z is a fictitious variable that slowly oscillates sinusoidally between the range of μ_1 indicated

in Figure 4(c). We define z as follows:

$$z := \bar{\mu}_1 - A \sin(\varepsilon t), \tag{4}$$

and used the average $\bar{\mu}_1 = -0.0395$, with amplitude $A = 0.0066$ and speed $\varepsilon = 0.01$. Fold/subHopf (pseudo-plateau) bursting can be obtained by choosing μ_2 above the point on HC where SNP ends, and below $\mathsf{BT}_r^{\text{far}}$ in Figure 4(c). An example with $\mu_2 = 0.5$ is shown in Figures 5(c) and (d). For $\mu_2 = 0.5$ the slow variable z oscillates around $\bar{\mu}_1 = -0.01$ with amplitude $A = 0.15$ and speed $\varepsilon = 0.1$.

For intermediate values of μ_2, in between DH and the point on HC where SNP ends in Figure 4(c), a transitional form of bursting with square-wave appearance is found in which the Hopf bifurcation is subcritical but becomes stable via an SNP before going homoclinic. The stable branch then carries the spikes of the active phase and the unstable branch has no influence. The canonical square-wave example that has introduced a generation of computational neuroscientists to bursting [20, Fig. 7.9] is of this type, albeit with the SNP outside the knees; it does not occur in the traditional slice shown in Figure 3 but rather appears as a transitional form between the classical supercritical fold/homoclinic and fold/subHopf types in the scenario of Figure 4.

For values of μ_2 that intersect the segment SNIC_l, no type of bursting is possible with one very slow variable but may be possible for non-small ϵ. Parabolic bursting would be possible with two (also very) slow variables. This has not been observed in pituitary cells, but the diagram is compatible with the beating (repetitive large spikes) seen spontaneously in lactotrophs and in somatotrophs when the large conductance voltage- and calcium-dependent (BK) channel is blocked [8].

From Figure 4, it seems that fold/subHopf bursting and its putative cousin fold/homoclinic bursting appear in the same unfolding of a codimension-three singularity, namely, the one that gives rise to the point $\mathsf{BT}_r^{\text{far}}$ and associated bifurcations SN_r and H. However, $\mathsf{BT}_r^{\text{far}}$ does not arise from a degenerate Bogdanov–Takens bifurcation and must be organized by another codimension-three singularity, perhaps one that is listed by Khibnik *et al.* [15]; we have not been able to characterize this singularity more precisely. We remark here that such a different codimension-three singularity is unlikely to give rise to a second saddle-node bifurcation SN_l, which is essential for both fold/homoclinic and fold/subHopf bursting.

All known bursters that appear simultaneously with fold/homoclinic bursting in the unfolding of the focus case of the degenerate Bogdanov–Takens point, together with fold/subHopf bursting do exist as part of an unfolding of the *doubly*-degenerate Bogdanov–Takens bifurcation. There are other known burst types, such as fold/fold-cycle with small limit cycles [22], that do not occur in either of the slices we have considered; it may be possible to find this and possibly all burst types in a neighborhood of the codimension-four doubly-degenerate Bogdanov–Takens bifurcation.

4   Conclusions

The development of the theory of bursting serves as a valuable case study of the interplay between biology and mathematics. The impetus to examine bursting in the first place came from the experimental observation of it in cells. The mathematical analysis allowed the assembly of diverse experimental phenomena into a beautiful and coherent theory of considerable explanatory power and in turn facilitated modeling by providing ready-to-use templates. Rapid progress was made possible by the prior existence of a body of theory cataloging the possible behaviors of planar systems without regard to bursting; the strong separation of time scales allowed this to be leveraged into a theory of bursting.

As we have seen, however, some common forms of bursting (e.g., pseudo-plateau and fold/fold with no or only vestigial limit cycles) depend on the separation of time scales not being too great, otherwise spikes would not be seen in the active phase. This has led to consideration of pseudo-plateau bursting as a form of mixed-mode oscillation, in which y and z are considered slow and x fast. This approach has advantages for some purposes, such as predicting *a priori* how many spikes occur per burst, and cases exist in which the traditional fast-slow method fails completely [29].

Also, non-planar fast subsystems are likely in cells because they have to serve a variety of functions under different conditions and, therefore, incorporate a non-minimal set of ion channels. Coupling of bursters also naturally generates higher-dimensional fast subsystems. Instructive examples of single [2] and coupled cells [3] have been described, but the surface has only been scratched.

Prior biological observation and modeling experience indicated that pseudo-plateau and square-wave bursting should be cousins. We showed here that these burst types can be found in close proximity to a codimension-three singularity that arises in a neighborhood of the codimension-four doubly-degenerate Bogdanov–Takens bifurcation. We have not been able to establish the precise nature of this codimension-three singularity, but believe that, by itself, it cannot generate all possible known burst types. Therefore, it seems likely that bursting cells explore a bifurcation landscape in a neighborhood of a codimension-four singularity.

Acknowledgments

References

[1] W. B. Adams and J. A. Benson, *The generation and modulation of endogenous rhythmicity in the* Aplysia *bursting pacemaker neurone R15*, Prog. Biophys. molec. Biol. **46**(1) (1985), 1–49.

[2] R. Bertram R, M. J. Butte, T. Kiemel, and A. Sherman, *Topological and phenomenological classification of bursting oscillations*, Bull Math Biol. **57**(3) (1995), 413–439.

[3] J. Best, A. Borisyuk, J. Rubin, D. Terman and M. Wechselberger, *The dynamic range of bursting in a model respiratory pacemaker network*, SIAM J. Appl. Dyn. Syst., **4** (2005), 1107-1139.

[4] T. R. Chay and J. Keizer, *Minimal model for membrane oscillations in the pancreatic β cell*, Biophys. J. **42** (1983), 181–190.

[5] L. Duan, Q. Lu, and Q. Wang, *Two-parameter bifurcation analysis of firing activities in the Chay neuronal model*, Neurocomputing **72** (2008), 341–351.

[6] F. Dumortier, R. Roussarie, and J. Sotomayor, *Generic 3-parameter families of planar vector fields, unfoldings of saddle, focus and elliptic singularities with nilpotent linear parts*, Springer Lect. Notes Math. **1480** (1991) 1489–1500.

[7] M. Golubitsky, K. Josić and T. J. Kaper, *An unfolding theory approach to bursting in fast-slow systems*, in "Global Analysis of Dynamical Systems", (eds. H. W. Broer, B. Krauskopf, and G. Vegter), Institute of Physics Publishing, (2001), 277–308.

[8] F. van Goor, Y.-X. Li, and S. S. Stojilkovic, *Paradoxical role of large-conductance calcium-activated K^+ (BK) channels in controlling action potential-driven Ca^{2+} entry in anterior pituitary cells*, J. Neurosci. **16**(16) (2001), 5902–5915.

[9] F. van Goor, D. Zivadinovic, A. Martinez-Fuentes, and S. Stojilkovic, *Dependence of pituitary hormone secretion on the pattern of spontaneous voltage-gated calcium influx. Cell type-specific action potential secretion coupling*, J Biol Chem **276**(36) (2001), 33840–33846.

[10] J. Hindmarsh and M. Rose, *A model of neuronal bursting using three coupled first order differential equations*, Proc. R. Soc. London **B221** (1984), 87–102.

[11] A. L. Hodgkin and A. F. Huxley, *A quantitative description of membrane current and its application to conduction and excitation in nerve*, J. Physiol. (London) **117** (1952), 205–249.

[12] F. C. Hoppensteadt and E. M. Izhikevich, "Weakly Connected Neural Networks", Springer-Verlag, New York, 1997.

[13] E. M. Izhikevich, *Neural excitability, spiking and bursting*, Intl. J. Bifurc. Chaos **10**(6) (2000), 1171–1266.

[14] J. Keener and J. Sneyd, "Mathematical Physiology," 2nd edition, Springer-Verlag, New York 2008.

[15] A. I. Khibnik, B. Krauskopf, and C. Rousseau, *Global study of a family of cubic Liénard equations*, Nonlinearity **11**(6) (1998), 1505–1519.

[16] A. P. LeBeau, A. B. Rabson, A. E. McKinnon, and J. Sneyd, *Analysis of a reduced model of corticotroph action potentials*, J. Theoretical Biol.**192** (1998), 319–339.

[17] M. Pernarowski, *Fast subsystem bifurcations in a slowly varying Liénard system exhibiting bursting*, SIAM J. Appl. Math. **54** (1994), 814–832.

[18] J. Rinzel *Bursting oscillations in an excitable membrane model*, in "Ordinary and Partial Differential Equations," (eds. B. D. Sleeman and R. D. Jarvis), Springer Lect. Notes Math. **1151** (1985), 304–316.

[19] J. Rinzel *A formal classification of bursting mechanisms in excitable systems*, in "Proc. Intl. Cong. Math. (ed. A. M. Gleason), American Mathematical Society (1987) 1578–1593).

[20] J. Rinzel and B. Ermentrout, *Analysis of Neural Excitability and Oscillations*, in "Methods in Neuronal Modeling" (eds. C. Koch and I. Segev), The MIT Press (1998) 251–291

[21] J. Rinzel and Y. S. Lee, *Dissection of a model for neuronal parabolic bursting*, J. Math. Biol. **25** (1987)653–675.

[22] A. Shilnikov, R. L. Calabrese, and G. Cymbalyuk, *Mechanism of bistability: Tonic spiking and bursting in a neuron model*, Phys. Rev. E **71** (2005), 056214.

[23] J. V. Stern, H. M. Osinga, A. LeBeau, and A. Sherman, *Resetting behavior in a model of burting in secretory pituitary cells: Distinguishing plateaus from pseudoplateaus*, Bull Math Biol. **70**(1) (2008), 68–88.

[24] J. Tabak, N. Toporikova, M. E. Freeman, and R. Bertram, Low dose of dopamine may stimulate prolactin secretion by increasing fast potassium currents, J. Comput Neurosci. **22**(2), (2007), 211-222.

[25] W. Teka, K. T. Tsaneva-Atanasova, R. Bertram, and J. Tabak, *From plateau to pseudo-plateau bursting: Making the transition*, Bull Math Biol., in press (PMID: 20658200).

[26] N. Toporikova, J. Tabak, M. E. Freeman, and R. Bertram, *A-type K^+ current can act as a trigger for bursting in the absence of a slow variable*, Neural Comput. **20**(2), (2008), 436–451.

[27] K. T. Tsaneva-Atanasova, H. M. Osinga, T. Rieß, and A. Sherman, *Full system bifurcation analysis of endocrine bursting models*, J. Theoretical Biology **264**(4) (2010), 1133–1146.

[28] K. T. Tsaneva-Atanasova, A. Sherman, F. van Goor, and S. S. Stojilkovic. *Mechanism of spontaneous and receptor-controlled electrical activity in pituitary somatotrophs: Experiments and theory* Journal of Neurophysiology, **98**(1) (2007), 131–144.

[29] T. Vo, R. Bertram, J. Tabak, and M. Wechselberger, *Mixed mode oscillations as a mechanism for pseudo-plateau bursting.* J Comput Neurosci. **28**(3) (2010), 443–58.

[30] G. de Vries, *Multiple bifurcations in a polynomial model of bursting oscillations*, J. Nonlinear Sci. **8** (1998), 281–316.